

---

# Jet Impingement Heat Transfer on a Plate with Axisymmetric Square Grooves - A Numerical Investigation

**Asem Nabadavis**

Department of Mechanical Engineering, Manipur Technical University, Imphal, India

**Dipti Prasad Mishra**

Department of Mechanical Engineering, BIT Mesra, Ranchi, India

*ABSTRACT - This investigation focusses on analysis of the nature of Nusselt number ( $Nu$ ) when an air jet strikes upon a grooved surface having a constant heat flux. The investigation is carried out by solving conservation equations of mass, momentum and energy with two equation-based  $k$ -epsilon turbulence model to determine the wall temperature and Nusselt number of the plate. The similar investigation was carried out where the surface was without any grooves [1]. The heat transfer characteristic for the grooved surface was investigated by varying  $H/d$  ratio when the Reynolds number of the jet ( $Re_j$ ) was fixed. The results of the flat surface investigation and the grooved surface investigation will be compared under a common parameter and analyzed.*

**Keywords—** Jet impingement heat transfer; CFD; ANSYS FLUENT, Grooved surface, Constant heat flux wall

## 1. INTRODUCTION

Jet impingement heat transfer has wide range of applications in various industries due to its high heat transfer coefficient at the stagnation region. There have been many studies on the jet impingement heat transfer with many different configurations such as flat plate with constant wall temperature, flat plate with constant heat flux wall, plates with axisymmetric grooves of different shapes etc. Experimental study carried out by B. Sagot et. al [2] using axisymmetric grooved wall found that gas-to-wall heat transfer enhancement in an impinging jet flow with axisymmetric grooves on the plate surface under constant wall temperature conditions has been studied. Square grooves have been found to be more efficient, for heat transfer intensification, than those with a triangular profile. The study also found that the heat transfer intensification was effective at regions nearby the stagnation region and it was valid for jet Reynolds number ( $Re_j$ ) in the region of 15000 to 30000. An experimental study was carried out by R.B. Kalifa et. al. [3] to analyze the behavior of a circular air jet impinging a flat plate subjected to a variable temperature. They found that the flow field is affected by varying the Reynolds number while maintaining the other parameters fixed. Also, an observation was made that the flow separation occurs farther the jet centerline for larger Reynolds numbers. H. Shariatmadar et al. [4] carried out experimental and numerical study on heat transfer characteristics of various geometrical arrangement of impinging jet arrays. The study found that the local heat transfer coefficient increases by increasing the Reynolds number and decreasing  $H/d$  of a particular arrangement of slot jet arrays. An experimental investigation was carried out by Anwarullah et, al. [5] to study the increase of heat transfer from surface of the electronic components by impingement of a circular air jet. It was found that, for a fixed Reynolds number, as  $H/d$  increases the local Nusselt number increased till  $H/d$  value of 4 and for higher values of  $Re_j$ , the local Nusselt number increased till  $H/d = 6$ . Kannan B.T. and Senthilkumar Sundararaj [6] studied the heat transfer characteristics on axisymmetric plate with and without grooves. Katti and Prabhu [7] investigated on axisymmetric detached ribs and different configurations of detached ribs were arranged axisymmetrically on the target plate. The influence of different rib parameters on the local distribution of heat transfer coefficients was also analysed and the results were compared with the radial heat transfer distribution between impinging jet and smooth surface.

Nabadavis and Mishra [1] carried out numerical investigation on jet impingement heat transfer on a flat plate with the same conditions i.e. constant wall heat flux,  $Re_j$  and the size of the computational domain. It was

found that maximum heat transfer characteristic was obtained at  $H/d = 25$  at  $Re_j = 20000$  and it was also observed that heat transfer rate increases with the increase of Reynolds number of jet.

## 2. MATHEMATICAL FORMULATION

The computational investigation is carried out for a jet with a nozzle diameter  $d$  which impinges on the target surface i.e. grooved surface having a diameter  $D$ . The nozzle distance from the target surface is  $H$ . The computational domain has a diameter of  $D_{CD}$  and a height of  $H_{CD}$  as shown in the Fig. 1. The flow field in the domain is computed using two-dimensional axis-symmetry incompressible Navier–Stokes equations with a two-equation  $k-\epsilon$  turbulence model along with the energy equation. The two-equation based  $k-\epsilon$  turbulence model is used as it is more reliable at higher Reynolds number for simulation of flow field (Angioletti et al. [5]).

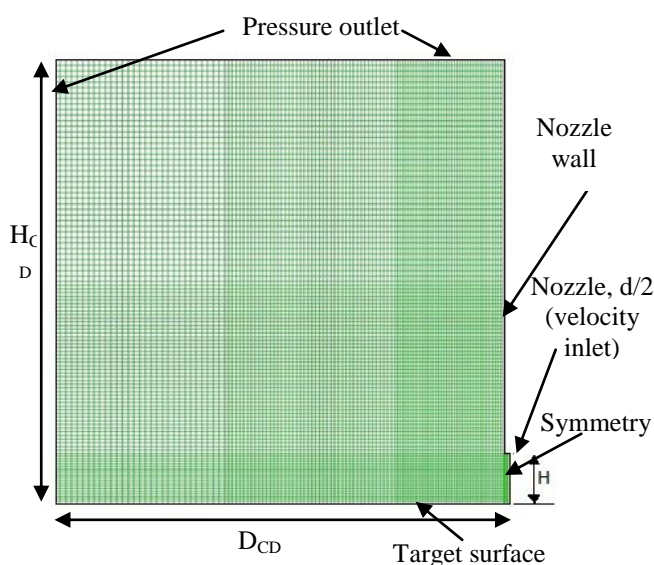


Fig.1.: Computational domain of Single Jet Impingement case without grooves

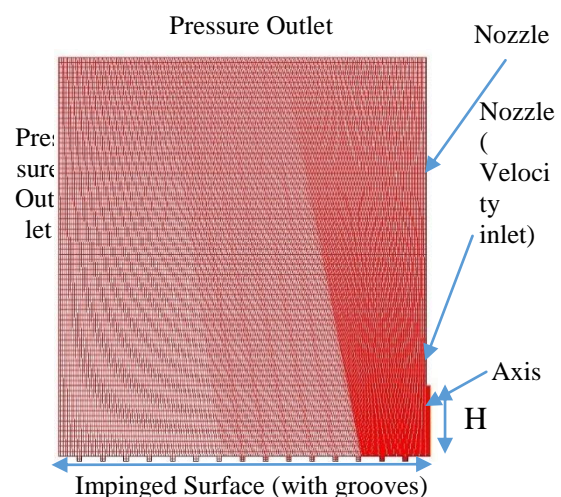


Fig. 2: Computational domain for a single jet with grooved surface

Air at temperature 300K is the fluid used for simulation process and the Reynolds number of the jet ( $Re_j$ ) is taken as 20000 and range is  $H/d$  is  $3 \leq H/d \leq 30$ . As the air density varies with temperature, the density of air has been computed according the ideal gas law. The dimensions of the grooves in the grooved surface has been taken as 1 mm depth, 1 mm width and 6 mm pitch.

### 2.1 Governing Equation

The governing equations for the above analysis can be written as:

Continuity equation:

$$\frac{\partial}{\partial x_i} (\rho U_i) = 0 \quad (1)$$

### 2.2 Momentum Equation:

$$\frac{D(\rho U_i)}{Dt} = \frac{\partial p}{\partial x_i} + \frac{\partial}{\partial x_j} \left[ \mu \left( \frac{\partial U_i}{\partial x_j} + \frac{\partial U_j}{\partial x_i} \right) - \rho \overline{u_i u_j} \right] \quad (2)$$

where  $p$  is the modified pressure ( $p + 2\rho k/3$ ) and  $\rho$  is the fluid density.

$$\frac{p}{\rho} = RT \quad (3)$$

where  $R$  is the characteristic gas constant = 0.287 kJ/kg K at 300 K.

### 2.3 Energy equation:

$$\frac{D(\rho T)}{Dt} = \frac{\partial}{\partial x_j} \left[ \left( \frac{\mu}{Pr} + \frac{\mu}{Pr_t} \right) \frac{\partial T}{\partial x_i} \right] \quad (4)$$

The density  $\rho$  is taken to be a function of temperature according to ideal gas law as per Equation (3), while dynamic viscosity  $\mu$  and thermal conductivity are kept constant.

#### *k-ε model:*

*Turbulence kinetic energy:*

$$\frac{D(\rho k)}{Dt} = D_k + \rho P - \rho \varepsilon \quad (5)$$

*Rate of dissipation of k:*

$$\frac{D(\rho \varepsilon)}{Dt} = D_\varepsilon + C_{1\varepsilon} \rho P \frac{\varepsilon}{k} - C_{2\varepsilon} \rho \frac{\varepsilon^2}{k} \quad (6)$$

$$\overline{u_i u_j} = \frac{2}{3} k \delta_{ij} - v_t \left( \frac{\partial u_i}{\partial x_j} + \frac{\partial u_j}{\partial x_i} \right), \quad v_t = 0.09 \frac{k^2}{\varepsilon} \quad (7)$$

$$D_\phi = \frac{\partial}{\partial x_i} \left[ \left( \mu + \frac{\mu_t}{\sigma_\phi} \right) \frac{\partial \phi}{\partial x_j} \right] \quad (8)$$

$$P = -\overline{u_i u_j} \frac{\partial u_i}{\partial x_j} \quad (9)$$

where  $\sigma_k$  and  $\sigma_\varepsilon$  are Prandtl numbers for  $k$  and  $\varepsilon$ . The constants used in the above  $k-\varepsilon$  equations are:

$$C_{1\varepsilon} = 1.44; C_{2\varepsilon} = 1.92; \sigma_k = 1.0; \sigma_\varepsilon = 1.3, Pr_t = 1.$$

### 2.4 Boundary Conditions

Figures (1, 2) show for surface with and without grooves respectively and the boundary conditions have been shown in Fig.2. The target surface has been given a constant heat flux of 5600 W/m<sup>2</sup>. An axisymmetric boundary condition has been employed for both cases. Velocity inlet has been given at the nozzle exit which gives high velocity air impinging at the flat surface and the surface that is to be impinged by the jet is taken as a wall. The domain limit has been treated as pressure outlet at atmospheric pressure.

$$p = p_a \quad (10)$$

In CFD simulation, the value of  $p_a$  has been taken as zero (0). The velocity at the outlet will be computed from the local pressure field so as to satisfy continuity, but all other scalar variables such as  $k$  and  $\varepsilon$  are computed from the zero-gradient condition. At the inlet, the turbulent intensity has been set to 2 percent and the turbulent viscosity ratio as 5 with the velocity known. And the backflow turbulent intensity at all the pressure outlet has been set to 5 percent but if there are no backflow at the pressure outlet then the value of  $k$  and  $\varepsilon$  are computed from the zero-gradient condition at the particular point.

### 2.5 Computation of Heat Transfer and Flow Parameters

The heat transfer and flow parameters are computed as given in Bu et al. [4]

Local convective heat transfer coefficient,

$$h_r = \frac{q}{T_{wr} - T_{in}} \quad (11)$$

where  $q$  is the heat flux on the flat plate;  $T_{wx}$  and  $T_{in}$  are the local temperature on the plate surface and inlet temperature of supplied air respectively.

Local Nusselt number,

$$Nu_r = \frac{h_r d}{k_{air}} \quad (12)$$

where  $d$  is the diameter of nozzle and  $k_{air}$  is thermal conductivity of air.

The jet Reynolds number,

$$Re_j = \frac{4G_m \times d}{\rho N \pi d^2 \left(\frac{\mu}{\rho}\right)} = \frac{4G_m}{N \pi d \mu} \quad (13)$$

$$G_m = \rho \cdot \frac{\pi d^2}{4} \cdot v_{in} \quad (14)$$

where  $G_m$  is mass flow rate of air and  $N$  is the number of jets,  $\rho$  is the density of air,  $\mu$  is the viscosity of air and  $v_{in}$  is the velocity at inlet.

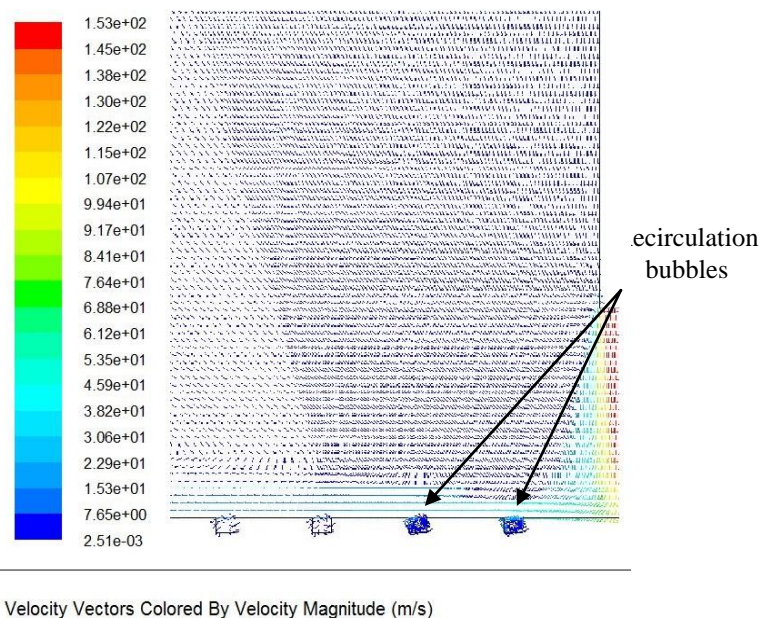


Fig. 3: Visualisation of velocity vectors of the fluid flow in grooved surface

## 2. NUMERICAL PROCEDURE

Three-dimensional equations (two-dimensional axis-symmetric for single jet) of mass, momentum, energy and turbulence have been solved, in case of multiple jet system, by the algebraic multigrid solver of Fluent 14 by using proper boundary conditions to satisfy the necessary conditions. A first order upwind scheme was considered for momentum, energy as well as turbulent discretized equations. For pressure-velocity coupling, SIMPLE (semi-implicit method for pressure-linked equation) algorithm was used for better convergence. Convergence of the discretized equations were said to have been achieved when all the residuals were below  $10^{-3}$  for  $u$ ,  $v$ ,  $w$ ,  $p$ ,  $k$  and  $\mathcal{E}$  whereas for energy the residual level was fixed at  $10^{-6}$ .

## 3. RESULTS AND DISCUSSIONS

### 3.1 Temperature Distribution Over the Plate

Following figure (Figure 4) is the temperature distribution over the plate with grooves at  $H/d = 3$  and  $Re_j = 20,000$  and Figure 5 is the local Nusselt number distribution over the plate. As we can see from the graph, temperature rise abruptly at the points between two grooves and hence lesser heat transfer at these points. This

is caused by the formation of recirculation bubbles which trap heat within them. Fig. 3 shows the recirculation bubbles within the grooves, which is due to air which get trapped in the grooves.

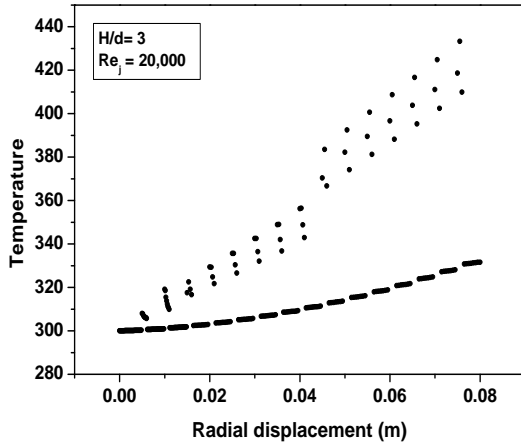


Figure 4: Temperature vs. radial distance plot for grooved surface at  $H/d = 3$  and  $Re_j = 20,000$

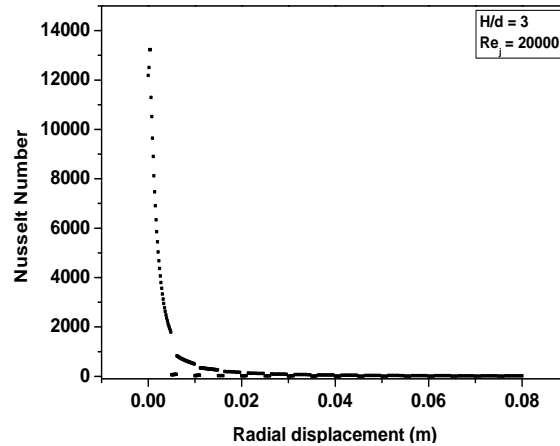


Figure 5: Nusselt number vs. radial distance plot for grooved surface at  $H/d = 3$  and  $Re_j = 20,000$

### 3.2 Variation of Nusselt number with Varying $H/d$ Value:

The local Nusselt number for jet impingement heat transfer on the grooved surface is shown in the Figure 6-9 for various values of  $H/d$ . From the graphs (Nusselt number vs Radial displacement) it can be seen that the Nusselt number is high in the stagnation region compared to the outer regions. The local Nusselt number in the stagnation region varies with the variation of  $H/d$ . From the graphs, as we increase  $H/d$  ratio the local Nusselt number decreases which implies that the heat transfer in the decreases in the stagnation region. But when the overall heat transfer rate is considered i.e when average Nusselt number is considered ( $Nu_{avg}$ ) maximum overall heat transfer occurs at  $H/d = 19$  as shown in Figure 10.

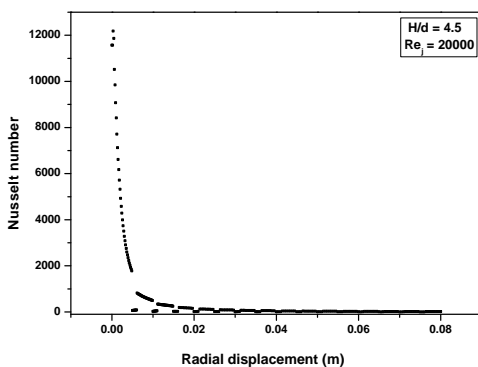


Figure 6: Nusselt number vs. radial distance plot for grooved surface at  $H/d = 4.5$  and  $Re_j = 20,000$

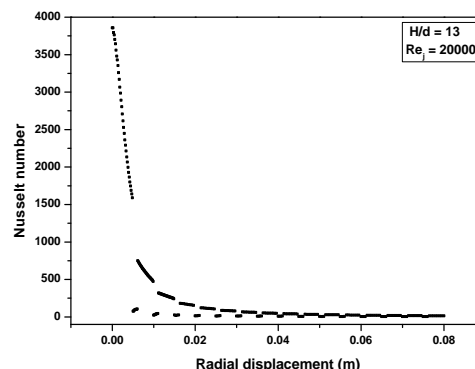


Figure 7: Nusselt number vs. radial distance plot for grooved surface at  $H/d = 13$  and  $Re_j = 20,000$

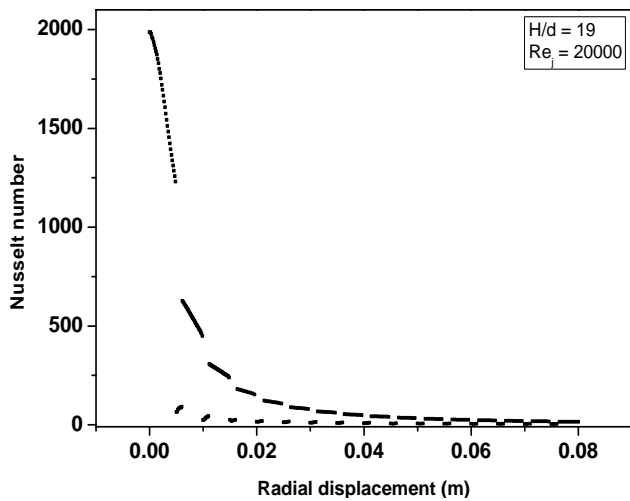


Figure 8: Nusselt number vs. radial distance plot for grooved surface at  $H/d = 3$  and  $Re_j = 20,000$

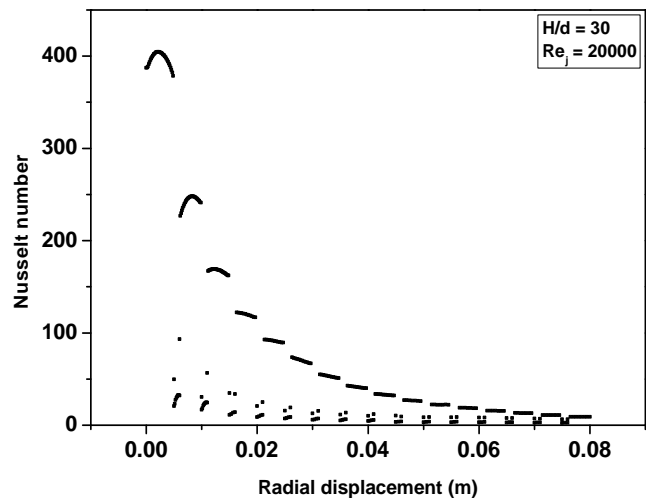


Figure 9: Nusselt number vs. radial distance plot for grooved surface at  $H/d = 3$  and  $Re_j = 20,000$

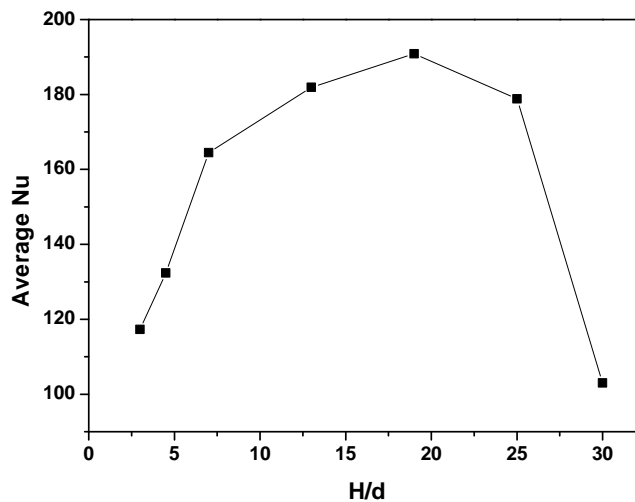


Figure 10:  $Nu_{avg}$  vs.  $H/d$  plot for a grooved surface at  $Re_j = 20,000$

### 3.3 Comparison Between Grooved Surface and Plane Surface

To find the more effective jet impingement heat transfer method between surface with and without groove, the heat transfer characteristics have been compared. Fig. 30 shows the temperature plot comparison of the two surfaces. It can be seen that the surface with grooves has lower temperature than the surface without groove except at some points i.e. at the point in the grooves. Temperature at the grooves rises abruptly when compared to the normal surface. This has been explained before in the previous section that recirculation bubbles within the grooves.

Recirculation bubbles tends to decreases the momentum of flow in the downstream region of the wall jet and it gives more time to extract heat from the wall surface. Due to this reason the temperature at the wall of surface with groove has lower temperature than the wall of the plane surface. To compare the overall heat transfer coefficient of plane surface and grooved surface, the

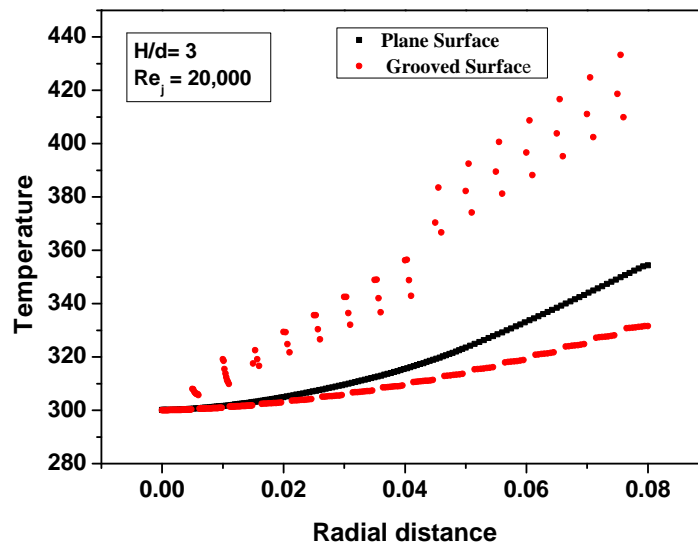


Fig. 11: Comparison of Temperature vs. Radial distance between grooved surface and plane surface at  $H/d = 3$  and  $Re_j = 20000$

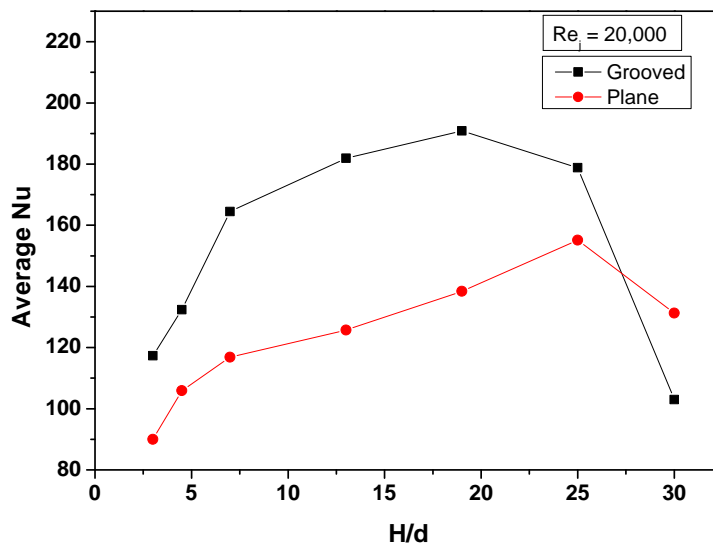


Figure 12: Comparison of  $Nu_{avg}$  between grooved surface and plane surface

average Nusselt number  $Nu_{avg}$  has been compared. Fig. 12 is the comparison of  $Nu_{avg}$  between the two surfaces. From Fig. 12, it can be seen that grooved surface has higher heat transfer rate than the plane surface at lower  $H/d$ . But when  $H/d = 30$  surface with groove has adverse effect on heat transfer rate giving lower heat transfer rate than plane surface. Hence, grooved surfaces are not advisable to be used for higher  $H/d$  values in jet impingement heat transfer.

#### 4. CONCLUSIONS

The following conclusions were taken after the thorough analysis of the results obtained in the ongoing investigation.

1. In grooved surface, temperature rise abruptly at the points between two grooves and hence lesser heat transfer at these points which is due to formation of recirculation bubbles which trap heat within them.
2. When a grooved surface was taken where the grooves has dimension of 1 mm depth, 1 mm width and 6 mm pitch at  $Re_j = 20,000$ , the maximum heat transfer is obtained at  $H/d = 19$  which has  $Nu_{avg} = 190.838$ . It was found that heat transfer increase 22.46 % when the grooved surface was used instead of a plane surface
3. It can be seen that grooved surface has higher heat transfer rate than the plane surface at lower  $H/d$ . But when  $H/d = 30$  surface with groove has adverse effect on heat transfer rate giving lower heat transfer rate than plane surface. Hence, grooved surfaces are not advisable to be used for higher  $H/d$  values in jet impingement heat transfer.

## REFERENCES

- [1] A Nabadavis and Dipti Prasad Mishra, 2016. “Numerical Investigation of Jet Impingement Heat Transfer on a Flat plate”, Carbon – Sci. Tech. 8/41-12
- [2] B. Sagot, G. Antonini, F. Buron, 2010. “Enhancement of jet-to-wall heat transfer using axisymmetric grooved impinging plates”. International Journal of Thermal Sciences 49/1026-1030
- [3] R.B. Kalifa, Sabra Habli, Nejla Mahjoub Saïd, Hervé Bournot, Georges Le Palec, 2016. “Parametric analysis of a round jet impingement on a heated plate”. International Journal of Heat and Fluid Flow 57/11–23
- [4] Hamed Shariatmadar, Shahab Mousavian, Mohammadkazem Sadoughi, Mehdi Ashjaee, 2016. “Experimental and numerical study on heat transfer characteristics of various geometrical arrangement of impinging jet arrays”. International Journal of Thermal Sciences 102/26-38
- [5] M. Anwarullah, V. Vasudeva Rao, K. V. Sharma, 2012. “Experimental investigation for enhancement of heat transfer from cooling of electronic components by circular air jet impingement”. Heat Mass Transfer 48/1627–1635
- [6] Kannan B.T. and Senthilkumar Sundararaj, 2015. “Steady state Jet Impingement Heat transfer from Axisymmetric Plates with and without Grooves”. Procedia Engineering, 127/25 – 32
- [7] Vadiraj Katti, S.V. Prabhu, 2008. “Heat transfer enhancement on a flat surface with axisymmetric detached ribs by normal impingement of circular air jet”, International Journal of Heat and Fluid Flow 29/1279–1294.